RMK 40

AN OPERATIONAL AIR POLLUTION MODEL USING ROUTINE METEOROLOGICAL DATA

Gunnar Omstedt

SMHI SWEDISH METEOROLOGICAL AND HYDROLOGICAL INSTITUTE

RMK 40

AN OPERATIONAL AIR POLLUTION MODEL USING ROUTINE METEOROLOGICAL DATA

Gunnar Omstedt

SMHI:s tryckeri 1984

Issuing Agency

SMHI
S-601 76 NORRKÖPING
Sweden

Report number
RMK 39

Report date
June 1984

Author (s)

Gunnar Omstedt

Title (and Subtitle)

AN OPERATIONAL AIR POLLUTION MODEL USING ROUTINE METEOROLOGICAL DATA

Abstract

An operational air pollution model using routine meteorological data is described. An hourly time series of pollutant concentrations is calculated for emissions from one or several tall industrial stacks. New methods developed by Nielsen et al. (1981), Berkowicz and Prahm (1982 a, b), Olesen et al. (1983) are used for determining boundary layer parameters i.e. surface sensible heat flux, friction velocity, mean wind speed and mixing height. These parameter values are used as input data to the dispersion part of the model. An updated Gaussian dispersion model, strongly supported by experimental data and similar to that developed by Weil and Bower (1982) is used. Briggs' dispersion parameters are used with the stability classification scheme based on the values of w_*/u during daytime and Pasquill-Gifford-Turner classes during nighttime for selection of stability classes. Plume rise and plume penetration of elevated stable layers are calculated by formulae from Briggs (1975). A similar model will also be used in Denmark (Berkowicz et al., 1983). Examples of results are given, based on four years of hourly meteorological data and radiosonde data from Bromma airport in Stockholm. A tentative comparison between the present model and Högström's (1968) model is made for emission from a 500 MW power plant. This comparison indicates that Högström's model predicts ground level concentrations that are too high occurring too close to tall industrial stacks.

Key words

Operational
Air pollution model
Gaussian dispersion model
Dispersion

Supplementary notes

Number of pages
59

Language
English

ISSN and title

0347-2116 SMHI Reports Meteorology and Climatology

Report available from:

Liber Grafiska AB/Förlagsorder
S-162 89 STOCKHOLM
SWEDEN

L I S T O F C O N T E N T S

		Page
1.	INTRODUCTION	1
2.	BOUNDARY LAYER PARAMETERS	2
2.1	Surface sensible heat flux	2
	2.1.1 The resistance method	3
	2.1.2 Net radiation	6
2.2	Surface flux of momentum	8
2.3.	Mean wind speed	9
2.4	Mixing height	9
3.	THE DISPERSION MODEL	13
3.1	Dispersion parameters	13
3.2	Stability classification	14
3.3	Buoyancy-enhanced dispersion	15
3.4	Plume rise	16
3.5	Plume penetration of elevated stable layers	18
4.	EXPERIMENTS AND RESULTS	20
4.1	Stability classification	20
4.2	Dispersion calculations	20
4.3	Högström's model	20
4.4	Future improvements of the model	26
5.	SUMMARY AND CONCLUSIONS	28
6.	ACKNOWLEDGEMENT	29
	REFERENCES	30
	APPENDIX A	

AN OPERATIONAL AIR POLLUTION MODEL USING ROUTINE METEOROLOGICAL DATA

1. INTRODUCTION

Air pollution dispersion models have been used for several decades for predicting air pollution impact from proposed and existing smoke stacks. In Sweden a model developed by Högström (1968) has been used since the 1960's. Since then considerable progress has been made in the understanding of the mechanisms controlling dispersion. The purpose of this work has therefore been to develop a new dispersion model more in line with present knowledge.

The model described in this report is similar to that developed by Berkowicz et al. (1983). The new model and Högström's model are both Gaussian plume models, but they differ in four major ways:

1. The treatment of meteorological input data.

2. The dispersion parameters used and the method for choosing their values.

3. The plume rise formulae.

4. The treatment of plume penetration of elevated stable layers.

In the new model only routine meteorological data are used. An hourly time series of pollutant concentrations is calculated for emissions from one or several tall industrial stacks. Thus, different types of air pollutant concentration statistics can be computed for e.g. comparison with air pollution standards. An example is the Swedish short-term air quality criterion for SO_2, which states that the SO_2-concentration measured over one hour must not exceed 750 $\mu g/m^3$ more than 1 percent of the time during a 30 day period.

2. BOUNDARY LAYER PARAMETERS

Air pollution dispersion is directly related to the mean and turbulent structure of the atmospheric boundary layer (ABL). If the ABL is in convective state, vigorous turbulence is maintained by buoyancy production and causes rapid mixing. Pollutants emitted from an elevated source can then be brought down to the ground close to the source resulting in high ground-level concentrations. In the stable ABL, turbulence is weak, driven by the wind shear and suppressed by buoyancy forces. If the emission is above the stable boundary layer it will remain at this layer forming a shallow pencil-like plume.

Air pollution dispersion is therefore strongly dependent on the time-varying meteorological conditions controlling the mean and turbulent structure of the boundary layer.

During daytime the solar heating of the ground results in an upward heat flux, producing convective turbulence. Turbulence can also be produced mechanically by wind shear resulting in a downward surface flux of momentum. Thus, mechanical as well as convective turbulence must be considered. As the boundary layer heats up, the boundary layer height gradually rises. In it turbulence is vigorous and limited by the boundary layer height.

Theoretical investigations by Deardorff (1972) and by Willis and Deardorff (1974) and atmospheric observations by Kaimal et al. (1976) have shown that for the convective boundary layer, the two most important parameters controlling turbulence are the depth of the convective boundary layer h and the convective velocity scale given by

$$w_* = \left(\frac{g}{T \rho C_p} H h\right)^{1/3} \qquad (1)$$

where H is the surface sensible heat flux,
h the boundary layer height,
g the constant of gravity,
ρ the air density,
T the air temperature and
C_p the specific heat of air at constant pressure.

The large convective eddies scale in size with h and the turbulence velocity scales (σ_v, σ_w) are proportional to w_*.

Stable boundary layers are complex, showing considerable variability in space and time. The knowledge of them is far less complete than that of convective boundary layer. From a practical point of view, however, stable boundary layers can be treated simply, because elevated sources yield their highest ground-level concentrations during convective conditions. During stable conditions the well-known Pasquill-Gifford-Turner scheme (Turner, 1964) for classification of stability is therefore used.

2.1 Surface sensible heat flux

The surface sensible heat flux is the main parameter determining the generation of convective turbulence. It can only be directly determined from expensive turbulent measurements. In long-term studies for different geographical areas methods using routine meteorological data, or for some places meteorological mast data, must be used.

If only routine meteorological data are available the sensible heat flux is calculated using a method developed by Berkowicz and Prahm (1982a). This method is presented in section 2.1.1 below.

If meteorological mast data are available a profile method developed by Berkowicz and Prahm (1982b) is used. This method requires, however, measurements of wind speed (at least at one level) and temperature difference between two levels.

2.1.1 The resistance method

The starting point is the equation for the surface energy balance

$$R_n = LE + H + G \qquad (2)$$

where R_n is the net radiation
LE the latent heat flux (flux of water vapor)
H the sensible heat flux and
G the soil heat flux.

The net radiation is the balance between downward and upward short-wave and long-wave radiation. Nielsen et al. (1981) have developed methods for estimation of net radiation by using routine meteorological data. These methods are used in the model and presented in section 2.1.2 below. In order to estimate the other three terms of (2) a method developed by Berkowicz and Prahm (1982a) is used. The latent heat flux is calculated by the Penman-Monteith equation.

The equation is

$$LE = \frac{(R_n - G)\, r_a(\Delta/\gamma) + Dq\, \rho\, C_p/\gamma}{r_s + (1 + (\Delta/\gamma))r_a} \qquad (3)$$

where Δ is the gradient of the saturated vapor pressure with respect to temperature and γ is the psychrometric constant.

These parameters are functions of temperature only. Dq is the humidity deficit in air defined as

$$Dq = q_s(T) - q \qquad (4)$$

where q_s is the saturated vapor pressure at the temperature T for a given reference height (screen height) and q is the actual vapor pressure at the same height.

The aerodynamical resistance r_a is the so called resistance of the atmospheric layer between a given reference height and the surface. In the surface layer, this resistance, although mainly determined by the momentum flux, is also determied by the heat flux. It can be expressed in terms of known flux profile relationships based on Monin-Obukhov's similarity theory (Monin and Obukhov, 1954).

For wind and temperature, we have

$$u(z) = u_*/k\left[\ln(z/z_o) - \psi_m(z/L) + \psi_m(z_o/L)\right] \quad (5)$$

$$T(z) - T(z_o) = R\Theta_*/k\left[\ln(z/z_o) - \psi_h(z/L) + \psi_h(z_o/L)\right] \quad (6)$$

where $\psi_m(z/L)$ and $\psi_h(z/L)$ are empirical stability correction functions. L is the Monin-Obukhov length given by

$$L = -\frac{\overline{T}\, u_*^3}{g\, k\, H}\, \rho\, C_p \quad (7)$$

where $\overline{T}$ is the average surface layer temperature
g the constant of gravity
k the von Karman constant
u_* the friction velocity and
H the sensible heat flux

R is a constant, and

$$\Theta_* = -\frac{H}{\rho\, C_p\, u_*} \quad (8)$$

To calculate the empirical stability corrections functions ψ_m and ψ_h the relationships based on the work by Businger et al. (1971) are used

$$\psi_m(z/L) = \ln\left[\left(\frac{1+x}{2}\right)^2\left(\frac{1+x^2}{2}\right)\right] - 2 \arctan x + \Pi/2 \quad (9)$$

$$x = (1 - 15\, z/L)^{1/4} \qquad \text{for } z/L < 0 \quad (10)$$

$$\psi_m(z/L) = -4.7\, z/L \qquad \text{for } z/L > 0 \quad (11)$$

$$\psi_h(z/L) = 2 \ln\left[\frac{(1+y)}{2}\right] \quad (12)$$

$$y = (1-9\, z/L)^{1/2} \qquad \text{for } z/L < 0 \quad (13)$$

$$\psi_h(z/L) = -(4.7/R)\, z/L \qquad \text{for } z/L > 0 \quad (14)$$

where R = 0.74 and the value of von Karman constant k = 0.35.

The aerodynamical resistance, r_a, for moisture and heat transfer is assumed to be equal and given by

$$r_a = \frac{T(z_o) - T(z_t)}{H/\rho\, C_p} \quad (15)$$

From (6), (8) and (15) the aerodynamical resistance can be written:

$$r_a = \frac{R}{k\, u_*} \left[\ln \frac{z_t}{z_o} - \psi_h(z_t/L) + \psi_h(z_o/L)\right] \qquad (16)$$

Eliminating u_*, by using (5), the final expression for the aerodynamical resistance is obtained

$$r_a = \frac{R}{k^2 u(z_u)} \left[\ln \frac{z_u}{z_o} - \psi_m(z_u/L) + \psi_m(z_o/L)\right] \qquad (17)$$
$$\cdot \left[\ln \frac{z_t}{z_o} - \psi_h(z_t/L) + \psi_h(z_o/L)\right]$$

where z_u and z_t are the levels where the wind speed and temperature are measured.

The surface resistance r_s is the resistance of the surface to water vapor transport. Following Berkowicz and Prahm (1982a) the surface resistance can be related to the humidity in the air (Dq), which acts as an indicator for the surface resistance, by the following equation:

$$r_s = (Dq/F)(\rho\, C_p/\gamma) \qquad (18)$$

where F is an empirical function of the surface moisture conditions.

For a vegetated surface the surface resistance is dependent on wetness conditions of the soil surface and on the degree of the stomata opening in the plants. As an indicator of the moisture conditions of the soil the accumulated net radiation since last precipitation (ΣR_n) is used.

The remaining part of the surface energy balance equation (2) is the soil heat flux. This term is modelled as a certain fraction of the sensible heat flux

$$G = \alpha H \qquad (19)$$

where α is a constant with a typical value of 0.3 for a grass covered surface.

The sensible heat flux can now be calculated from (2), (3) and (19) by the following equation

$$H = \frac{R_n(r_a+r_s) - Dq(\rho\, C_p/\gamma)}{r_s+(1+\Delta/\gamma))r_a+\alpha(r_a+r_s)} \qquad (20)$$

Equations (17) and (20) are solved simultaneously by an iterative method (Berkowicz and Prahm, 1982b).

The resistance method has been tested against data from Denmark (Højbackegård), Sweden (Marsta) and Holland (Cabau) with good results. For further details see Berkowicz and Prahm (1982a).

2.1.2 Net radiation

The methods developed by Nielsen et al. (1981) are followed. From 5 years of hourly data at one site in Denmark (Højbakkegård) empirical relations for net radiation over green grass were derived. At some meteorological stations incoming short-wave radiation S_d is measured. When such measurements are available net radiation can be calculated by the following equation:

$$R_n = (1 - \alpha_g)/(1 + \beta)\ S_d + L_{no}\ (N) \qquad (21)$$

where α_g is the surface albedo. L_{no} is an estimated constant for given total cloud cover N. L_{no} is related to the net long-wave radiation L_{net} at the ground. β is the heating coefficient equal to $-dL_{net}/dR$ (Monteith and Szeicz, 1961).

Estimated values of $(1-\alpha_g)/(1+\beta)$ and $L_{no}(N)$ are shown in Table 1 and regression lines in Figure 1. A representative surface albedo value for these measurements was 0.25. Generalization to other surfaces can be made by using representative albedo values and assuming the same heating coefficient β.

When no direct measurements of S_d are at hand net radiation is calculated from observations of total cloud cover, cloud type and solar radiation by following equation:

$$R_n = a_0 + a_1 \sin\Theta + a_2 \sin^2\Theta + a_3 \sin^3\Theta \qquad (22)$$

where Θ is the solar elevation and a_0, a_1, a_2, a_3 are empirical coefficients depending on surface albedo, cloud cover and types.

Cloud types are taken into account if the reported clouds are mainly of cirrus forms. A modified cloud cover N_m is introduced. If dominating cloud cover is high its weight is reduced by the following algorithm:

$$\begin{aligned} &\text{if } N < 3 \text{ then } N = N \\ &\text{if } N = 3 \text{ then } N = 2 \qquad (23) \\ &\text{if } N > 3 \text{ then } N = N - 2 \end{aligned}$$

Estimated values of a_0, a_1 and a_3 are shown in Table 2 and regression lines in Figure 2. The term with $\sin^2\Theta$ in equation (22) was insignificant and therefore excluded.

The solar elevation Θ for a given time and location is calculated by a simplified well-known astronomic formula from Robertson and Russel (1968).

The net radiation equations (21) and (22) have been tested against 10 years of data at another site in Denmark (Karup) with good results (Nielsen et al., 1981). They have also been compared with six days of data at a site in Sweden (Klockrike) with another surface albedo. The agreement even for this small time period was good.

N	L_{no} W/m^2	$(1-\alpha g)/(1+\beta)$
0	-95.0	.73
1	-89.2	.72
2	-78.2	.72
3	-67.4	.72
4	-57.1	.72
5	-45.7	.70
6	-33.2	.70
7	-16.5	.69
8	- 4.3	.69

Table 1 *Estimated values of L_{no} and $(1-\alpha g)/(1+\beta)$ (Eq. 21) for different cloud covers N in oktas (from Nielsen et al., 1981).*

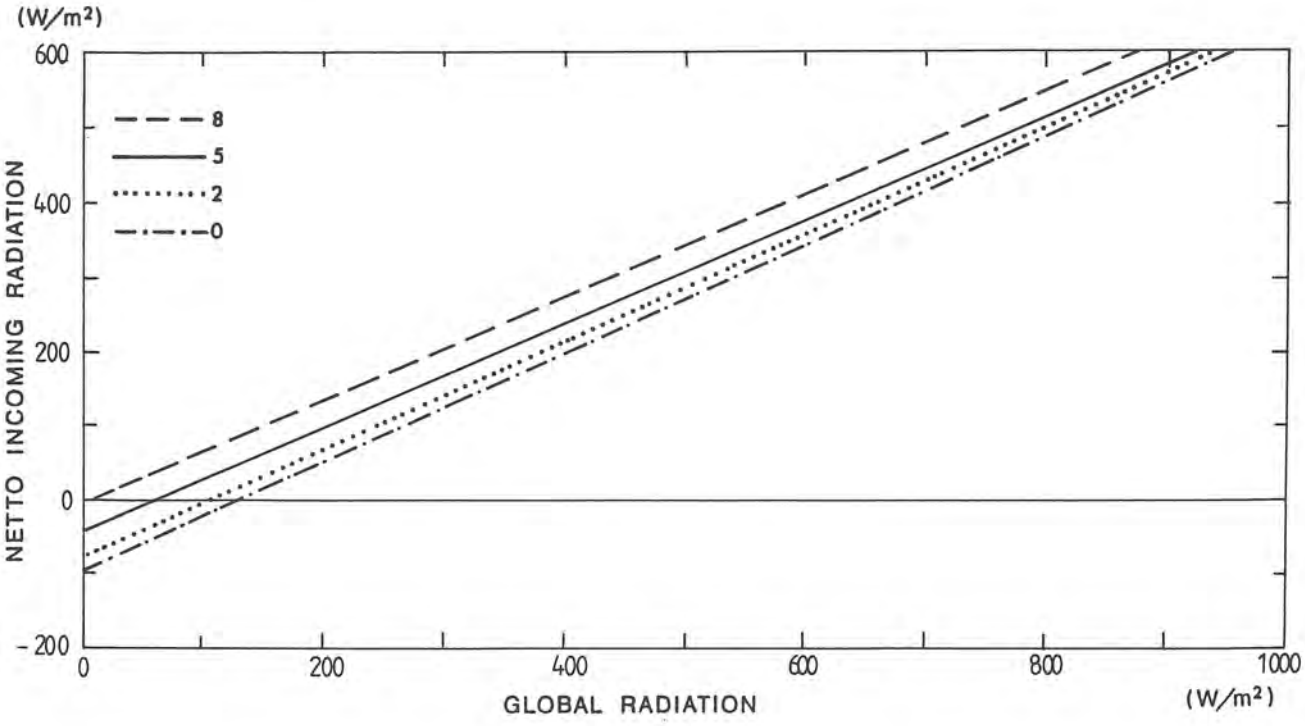

Figure 1 *Regression lines for the relation between R_n and S_d, (Eq. 21) for different total cloud covers in oktas (from Nielsen et al., 1981).*

N_m	a_0 W/m^2	a_1 W/m^2	a_2 W/m^2
0	-112.6	653.2	174.0
1	-112.6	686.5	120.9
2	-107.3	650.2	127.1
3	- 97.8	608.3	110.6
4	- 85.1	552.0	106.3
5	- 77.1	511.3	58.3
6	- 71.2	495.4	-37.9
7	- 31.8	287.5	94.0
8	- 13.7	154.2	64.9

Table 2 *Regression coefficients for* $R_n = a_0 + a_1 \sin\Theta + a_3 \sin^3\Theta$ *(Eq. 22) as a function of total modified cloud cover* N_m *(Eq. 23) (From Nielsen et al., 1981).*

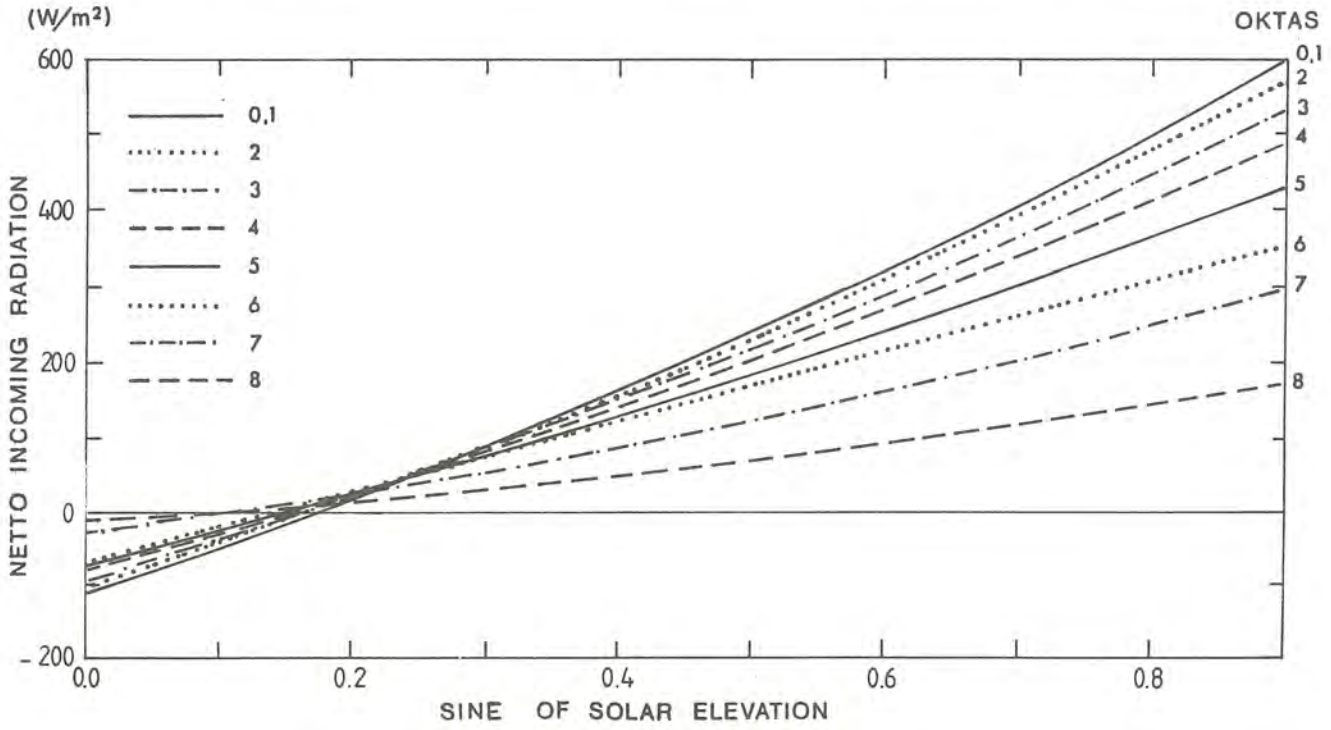

Figure 2 *Regression lines for different total modified cloud cover* N_m. *(From Nielsen et al,. 1981).*

2.2 Surface flux of momentum

The mechanical generation of turbulence is determined by the surface flux of momentum τ and given by

$$\tau = \rho u_*^2 \qquad (24)$$

where ρ is the density of air and
u_* is the friction velocity.

Friction velocity is related to wind speed u(z) at the height z (usually z = 10m) and the surface roughness parameter z_o by equation (5) i.e.

$$u(z) = u_*/k[\ln(z/z_o) - \psi_m(z/L) + \psi_m(z_o/L)]$$

where the empirical stabiliy corrections function ψ_m is given by equation (9), (10) and (11). The surface roughness parameter z_o characterizes the dynamical roughness of the ground and is related to the physical nature of the surface structure. Typical values of z_o are given in Table 3. A zero displacement level can be introduced in equation (5), by replacing z with z-d. For natural crop covered surface d can be estimated as 2/3 of the mean height of roughness elements (Brutsaert, 1975).

2.3 Mean wind speed

Atmospheric measurements in the convective boundary layer (Kaimal et al., 1976) show that almost all the gradient in mean wind speed is confined to a shallow region close to the ground, below 0.1 h, where h is the boundary layer height. Above that level mean wind speed is nearly uniform. Mean wind speed is therefore calculated for $z \leq 0.1$ h by using Monin-Obukhov's similarity equation (5) with the empirical correction functions given by equations (9) and (10). For $z > 0.1$ h the calculated wind speed at 0.1 h is used as a vertical average wind speed value. Weil and Brower (1983) have shown that this way of calculating wind profiles in the convective boundary layer provides a good fit to observed values.

If the boundary layer is slightly stable, i.e. small positive values of z/L, wind profiles in the surface layer are calculated by using the similarity equation (5) with the empirical correction function given by (11). For very stable conditions i.e. large positive values of z/L this method cannot be used because equation (11) results in unlimited increase of the mean wind speed with height. A critical stability number must be introduced (Berkowicz and Prahm, 1982b). If this number is violated wind speed is calculated at a given level (stack height) by using the measured wind speed (usually at 10m) times a constant factor.

2.4 Mixing height

The boundary layer height, or as it is often called, the mixing height, is an important parameter in an air pollution model. It determines whether or not a plume will be trapped inside the mixed layer. It is also an important parameter determining the internal turbulent structure of the boundary layer. This parameter is, however, not easy to determine on a routine basis because of the lack of data in the vertical.

The convective boundary layer shows a strong day-time development. It is often capped by an inversion. As the boundary layer heats up during the course of a sunny day, the inversion base gradually rises because the turbulence in the boundary layer entrains the warm air above the inversion base. Within the boundary layer and above 0.1 h, where h is the mixing height, mean potential temperature is relatively uniform. In the inversion layer potential temperature rapidly increases with height to the value in the overlying non-turbulent stable air.

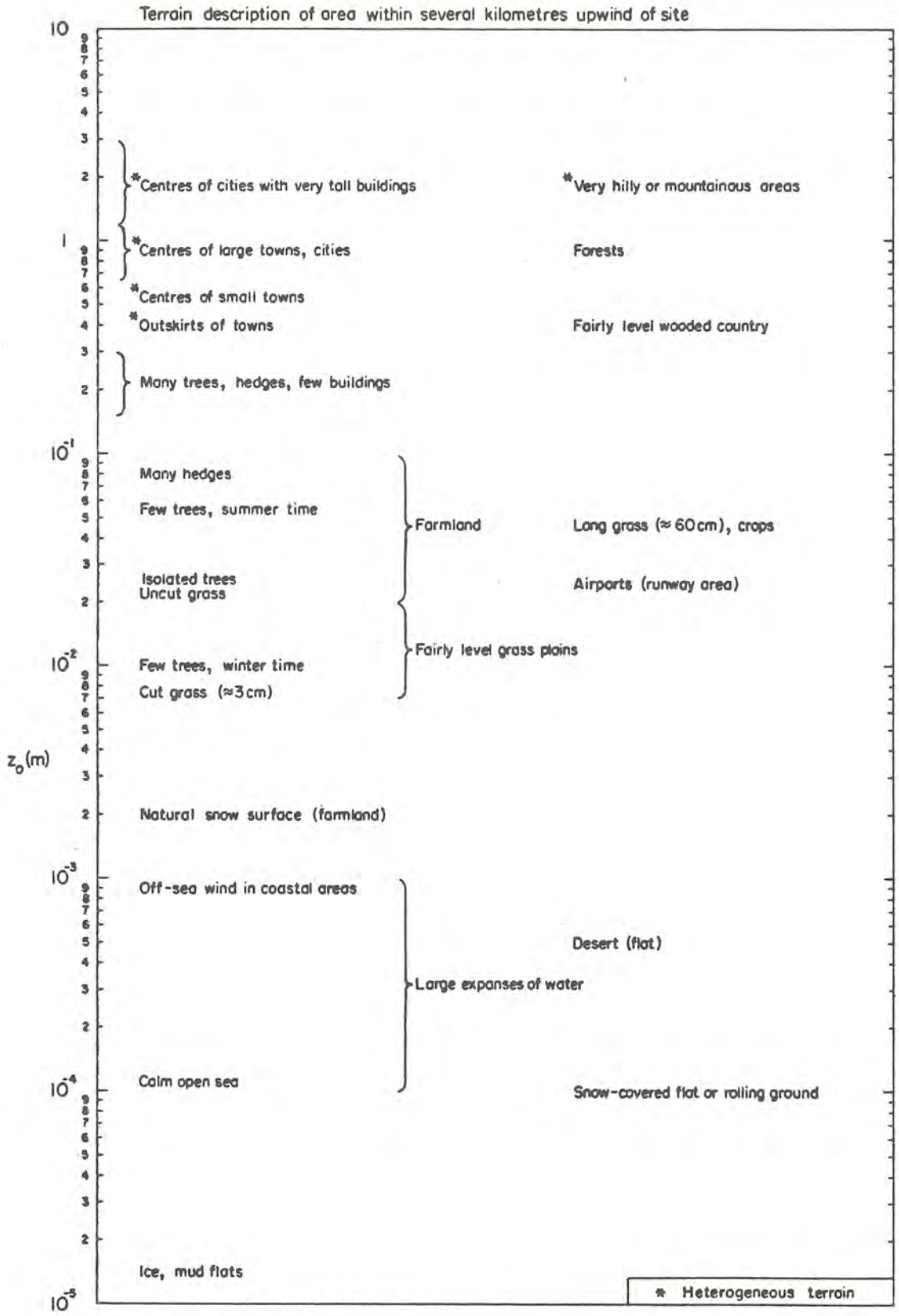

Table 3 Typical value of the surface roughness parameter z_0 (from Engineering Science Data Item Number 72026).

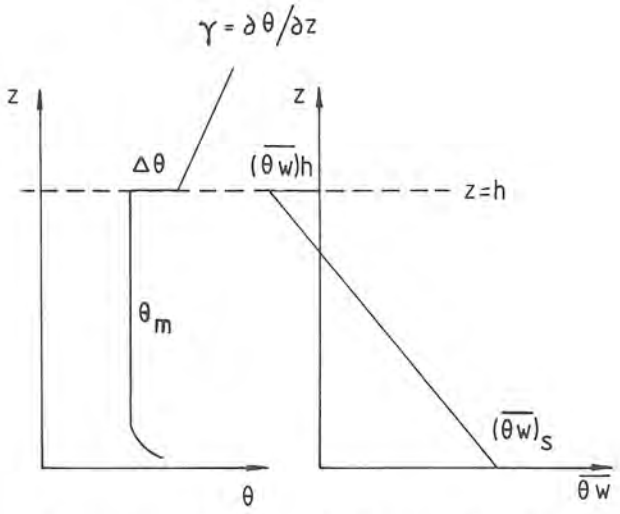

Figure 3 *A schematic picture of the vertical distributions of potential temperature and turbulent heat flux in and above a convective mixed layer.*

In Figure 3 a schematic picture of these observations is shown. The inversion layer is considered thin enough to be represented by a discontinuity in potential temperature.

Making use of Figure 3, ignoring horizontal advection, large-scale subsidence, radiation and latent heat effects, Tennekes (1973), has derived following equations:

$$\frac{d\Theta_m}{dt} = (\overline{\Theta w}_s - \overline{\Theta w}_h)/h \qquad (25)$$

$$\frac{d\Delta\Theta}{dt} = \gamma \frac{dh}{dt} - \frac{d\Theta_m}{dt} \qquad (26)$$

$$-\overline{\Theta w}_h = \Delta\Theta \frac{dh}{dt} \qquad (27)$$

where h is the mixing height,
Θ_m is the potential temperature
the subscripts 's' and 'h' refer to the surface and mixing height respectively.
The other notation is given in the figure.

To solve equations (25)-(27) they have to be closed by a parameterization of the turbulent kinetic energy budget. Several possibilities have been proposed (Tennekes and Driedonks, 1981).

By using an extensive set of field data, Driedonks (1982) has shown that good results can be obtained by using the following entrainment formula:

$$-\overline{\Theta w}_h = A\,\overline{\Theta w}_s + A_m \cdot u_*^3\, T_o/gh \qquad (28)$$

with $A = 0.2$ and $A_m = 5.0$.

From eq (25)-(28) the following equations can be derived

$$\frac{dh}{dt} = \frac{1}{\Delta\Theta}\left[0.2\,\overline{\Theta w}_s + 5\,\frac{u_*^3\,T_o}{g\cdot h}\right] \qquad (29)$$

$$\frac{d\Delta\Theta}{dt} = \left[\frac{0.2\gamma}{\Delta\Theta} - \frac{(1+0.2)}{h}\right]\overline{\Theta w}_s + \left[\frac{\gamma 5}{\Delta\Theta} - \frac{5}{h}\right]\frac{u_*^3\,T_o}{g\cdot h} \qquad (30)$$

Equations (29)-(30) describe completely the dynamics of h and $\Delta\Theta$. As initial conditions a simplified model from Carson (1973), similar to that described above, is used.

$$h^2(t) = \frac{2(1+2A)}{\gamma}\int_{t_o}^{t}\overline{\Theta w}_s\,dt \qquad (31)$$

$$\Delta\Theta(t) = \frac{\gamma h(t)\cdot A}{1+2A} \qquad (32)$$

where t_o is taken as the first time the surface sensible heat flux becomes positive (upward).

Olesen et al. (1983) have combined the above equations with data from radio soundings. This procedure is followed. The 00 GMT sounding is used to start the integration. The sensible heat flux is calculated by using the resistance method described above (section 2.1.1). When the sensible heat flux first becomes positive (upward) the daytime convective mixing height is calculated hourly by using equations (29)-(32). At 12 GMT the sounding from that time is introduced. A comparison is made between calculated mixing height and observed height, defined as the height to the first stable layer determined from the sounding. If a substantial difference occurs a correction is made for all the previous calculated mixing height values. The further integration proceeds from the 12 GMT profile. A comparison is also made between the 00 and 12 GMT soundings to ensure that the advection is not too extreme.

When conditions during daytime do not permit the use of the convective model a neutral mixing height is used given by

$$h = 0.25\,u_*/f \qquad (33)$$

where f is the Coriolis parameter, which is proportional to the earth's rotation rate and latitude.

The height of the stable boundary layer is at present calculated in a simplified way by using the neutral formula (33) with a lower bound of 150 m. An alternative is to use an empirical equation suggested by Venkatram (1980):

$$h = 2.4\cdot 10^3\,u_*^{3/2}$$

3. THE DISPERSION MODEL

The Gaussian plume model is the one most commonly used in practical applications for predicting air pollution impact from smoke stacks. Simple non-Gaussian models have recently been developed by Misra (1982), Venkatram (1983), Weil and Furth (1981). These models have, however, not been used, to any great extent, in practical applications because they refer to passive release while most real releases are associated with buoyancy. Weil and Brower (1982) have in a Gaussian plume model incorporated parameters that are in line with present knowledge of the convective boundary layer. The model is strongly supported by experimental data. It predicts dispersion of buoyant plumes from tall industrial stacks in flat terrain. Tall stacks are here defined as those with effective stack heights greater than 0.1 h, where h is the mixing height. A similar model will be used here. A description of the Gaussian equation and the two different grid systems used is given in Appendix A.

3.1 Dispersion parameters

Available empirical methods for predicting plume dispersion as a function of distance from the source and meteorological variables are based on a few carefully performed diffusion experiments. The Prairie Grass Experiment (Haugne, 1959) is probably the most well-known. Release was done from near ground level in a flat terrain. From these data the well-known Pasquill-Gifford (1961) dispersion curves were formulated. In Sweden Högström (1964) performed a diffusion experiment at Studsvik and Ågesta with release heights of 24, 87 and 50 meters basically during neutral and stable meteorological conditions. For tall sources the diffusion experiments made by Brookhaven National Laboratory (BNL) (Singer and Smith, 1966) and by the Tennessee Valley Authority (TVA) (Carpenter et al.,1970) were used to formulate the BNL and TVA dispersion curves. The BNL curves are based on non-buoyant tracer releases from a 104 meter tower, while the TVA curves are based on data from buoyant power plant plumes. Briggs analyzed the Pasquill, BNL and TVA curves and deduced a new set of curves (Gifford, 1975) which gave proper weight to the BNL and TVA data when these deviated from the Pasquill values. These empirical parameters are used in the present model and are given in Table 4.

Class	σ_y(m)	σ_z(m)
A	$0.22x(1 + 0.0001x)^{-1/2}$	$0.20x$
B	$0.16x(1 + 0.0001x)^{-1/2}$	$0.12x$
C	$0.11x(1 + 0.0001x)^{-1/2}$	$0.08x(1 + 0.0002x)^{-1/2}$
D	$0.08x(1 + 0.0001x)^{-1/2}$	$0.06x(1 + 0.0015x)^{-1/2}$
E	$0.06x(1 + 0.0001x)^{-1/2}$	$0.03x(1 + 0.0003x)^{-1}$
F	$0.04x(1 + 0.0001x)^{-1/2}$	$0.016x(1 + 0.0003x)^{-1}$

Table 4 *Briggs' dispersion parameters σ_y and σ_z as a function of downwind distance x(m).*

3.2 Stability classification

In order to select the appropriate dispersion curve, the turbulent state of the atmospheric boundary layer must be considered. Before going into details some principal results from recent studies of the atmospheric boundary layer are discussed. Theoretical investigations by Deardorff (1972) and by Willis and Deardorff (1974) have shown that the most important parameters controlling turbulence in the upper 90 percentage of the convective boundary layer are the convective velocity scale w_* and the mixing height h. The convective velocity scale is given by equation (1) above. In the upper part of the boundary layer (above 0.1 h) the turbulent velocity scales σ_w and σ_v are proportional to the convective velocity scale, while the most energetic eddies are determined by the mixing height.

Turbulence may also be mechanical in origin. On windy and overcast days mechanical turbulence will dominate. Mechanical turbulence is generated in the shear dominated surface layer. This layer does not extend much higher than $z = |L|$ where L is the Monin-Obukhov's length given by equation (7) above.

Since the mixed layer depth, h, represents the maximum extent of convective turbulence, the ratio

$$\frac{-L}{h} = \frac{1}{k}\left(\frac{u_*}{w_*}\right)^3 \qquad (34)$$

gives a measure of the relative importance of mechanically and convectively produced turbulence. This parameter can thus be thought of as a stability parameter. By assuming that the friction velocity u_* is a function of the mean wind speed, the stability parameter -L/h can be replaced by u/w_*. This ratio is used by Weil and Brower (1982) for the definition of stability during daytime conditions. If $u/w_* \leq 6$ turbulence in the mixed layer above 0.1 h will be dominated by convection (Deardorff and Willis, 1974).

To relate turbulence to diffusion Taylor's (1921) classical results on the spread of a continuous point source plume in homogeneous turbulence are used. In the limit of small travel time, or distance x, the dispersion coefficients can be written

$$\sigma_z = (\sigma_w/u)x \qquad (35)$$
$$\sigma_y = (\sigma_v/u)x$$

where σ_w and σ_v are the root-mean-square turbulent velocities in the vertical and crosswind directions respectively and u is the mean wind speed.

Briggs' short distance limits for σ_y and σ_z (see Table 4) exhibit the same dependence on x as equation (35). These are used by Weil and Brower (1982) in the following way to derive the range of u/w_* values.

The turbulent velocity scales, σ_w and σ_v are related to the basic parameters w_* and u_*. In the limiting case of convection dominated mixed layer, results from field measurement of Kaimal et al. (1976) are used.

These results show that in the upper 90 percentage of the mixed layer the turbulence velocities are given by

$$\sigma_w = \sigma_v = 0.56\ w_* \qquad (36)$$

In the limit of neutral conditions turbulence velocity scales consistent with Briggs' neutral (D) curves are used. Assuming $u_* = 0.05\ u$ the Briggs' D-curve implies that

$$\begin{aligned} \sigma_w &= 1.2\ u_* \\ \sigma_v &= 1.6\ u_* \end{aligned} \qquad (37)$$

For situations with combined mechanical and convective turbulence the total turbulent energy is expressed as a sum of two parts.

$$\sigma^2 = \sigma_M^2 + \sigma_C^2 \qquad (38)$$

where σ_M is the mechanically generated part and
σ_C is the convectively generated part.

Substituting equations (36), (37) into equation (38)

$$\begin{aligned} \sigma_w &= ((0.56\ w_*)^2 + (1.2\ u_*)^2)^{1/2} \\ \sigma_v &= ((0.56\ w_*)^2 + (1.6\ u_*)^2)^{1/2} \end{aligned} \qquad (39)$$

From (35) the following equations are obtained

$$\sigma_z = ((0.56\ w_*)^2 + (1.2\ u_*)^2)^{1/2} \qquad (40)$$

$$\sigma_y = ((0.56\ w_*)^2 + (1.6\ u_*)^2)^{1/2} \qquad (41)$$

Equations (40) and (41) with $u_* = 0.05\ u$ are used to define w_*/u values appropriate to Briggs' dispersion curves. These values are shown in Table 5.

The method described above can only be used for conditions with positive surface sensible heat flux. When the heat flux is negative the well-known Pasquill-Gifford-Turner (PGT) classification scheme (Turner, 1964) is used to define atmospheric stability (class D, E and F). An appropriate Briggs' curve is chosen based on calculated hourly PGT class.

3.3 Buoyancy-enhanced dispersion

Turbulence is also generated by the hot buoyant plume itself. To include this effect the dispersion parameters are modified according to a suggestion by Pasquill (1976) in the following way:

$$\sigma_z = \left[\sigma_{z\ pass}^2 + (\Delta h/3.5)^2\right]^{1/2} \qquad (42)$$

$$\sigma_y = \left[\sigma_{y\ pass}^2 + (\Delta h/3.5)^2\right]^{1/2} \qquad (43)$$

σ_y and σ_z represent the total vertical and horizontal spread the index 'pass' denotes the passive growth due to atmospheric turbulence (Briggs' curve) and Δh is the final plume rise.

Class	$\frac{w_*}{u}$
A	$0.286 < \frac{w_*}{u}$
B	$0.168 < \frac{w_*}{u} \leq 0.286$
C	$0.072 < \frac{w_*}{u} \leq 0.168$
D	$\frac{w_*}{u} \leq 0.072$
E	PGT
F	PGT

Table 5 *Range of w_*/u corresponding to Briggs' dispersion curve (Table 4). The Pasquill-Gifford-Turner classification is used when the surface sensible heat flux is negative.*

3.4 Plume rise

Most air pollution emitted by smoke stacks is associated with excess temperature and momentum causing the plume to rise above the top of the stack. This effect is very important in determining ground level concentrations. Maximum ground-level concentration is roughly proportional to the inverse square of the effective source height. An increase of the effective source height by e.g. a factor of two therefore decreases the maximum ground-level concentration by a factor of about four.

A lot of different models for plume rise prediction have been proposed. The reader is referred to Briggs (1975) for a review of available models. Most of the models employed are, however, only based on observations of plumes in stable or neutral boundary layers. For a convectively mixed layer the occurrence of plume looping associated with convective updrafts and compensating downdrafts also makes the concept of plume rise rather complicated.

In this model the final plume rise is calculated by formulae from Briggs (1975). The reader is referred to this reference and to the report by Weil and Brower (1982) for the detailed derivations of these formulae. A summary together with the final formulae used in the model will be given here.

For neutral and convective conditions the final plume rise Δh is calculated as the lower of the rises predicted by either Briggs 'break up' or 'touch down' model. In the 'break up' model plume rise is assumed to terminate when the effective turbulence dissipation rate of the plume equals that of the surrounding air. The turbulent dissipation rate in the surrounding air is given by Briggs for two cases i.e. for neutral and convective conditions.

For neutral (windy) conditions the resulting plume rise formula is

$$\Delta h = 1.3 \frac{F}{u\, u_*^2} (1 + h_s/\Delta h)^{2/3} \qquad (44)$$

where u is the wind speed at plume height,
u_* is the friction velocity,
h_s the stack height and
F is the buoyancy flux given by

$$F = \frac{V_g}{\Pi} \frac{g}{T_q} (T_q - T_a) \qquad (45)$$

where V_q and T_q are the volume flux and temperature at stack exit and T_a is the ambient air temperature.

For convective conditions the resulting formula is

$$\Delta h = 4.3 \left(\frac{F}{u}\right)^{3/5} H_*^{-2/5} \qquad (46)$$

where $H_* = gH/(C_p\, \rho\, T_a)$
H is the sensible heat flux,
g the gravitational acceleration
T_a the ambient air temperature,
ρ the air density and
C_p the specific heat of air at constant pressure

In the 'touch down' model the buoyant plume is assumed to rise relative to a region of convective downdraft with the velocity of the downdraft exceeding the rise velocity due to plume buoyancy, bringing the plume to the ground. This can happen during strong convective conditions. The final plume rise is

$$\Delta h = (F/(u\, w_d^2))(1 + (2\, h_s/\Delta h))^2 \qquad (47)$$

where w_d is the mean downdraft velocity given by

$$w_d = 0.4\, w_*$$

The three different formulae for final plume rise given above (eq (44), (46) and (47)) were derived for three different conditions. In a given application each condition or formula must be considered. The most limiting one, i.e. the formula that gives the lowest plume rise, is selected as the final plume rise for neutral or convective conditions.

For stable conditions the final plume rise is calculated by

$$\Delta h = 2.6\left(\frac{F}{u \cdot s}\right)^{1/3} \qquad \text{in windy conditions} \qquad (48)$$

$$\Delta h = 5\,\frac{F^{1/4}}{s^{3/8}} \qquad \text{in calms} \qquad (49)$$

where $s = \frac{g}{T_a}\,\frac{\partial \Theta}{\partial z}$

and $\frac{\partial \Theta}{\partial z}$ is the ambient air potential temperature gradient.

The final rise is given by the least of the rises predicted by eq (48) and (49).

3.5 Plume penetration of an elevated stable layer.

If a plume is sufficiently buoyant it can partially or completely penetrate into the stable air capping the mixed layer. Ground-level concentrations can then be dramatically reduced. If the plume is not sufficiently buoyant, the plume is trapped into the mixed layer. In combinations with low wind speeds, this can give rise to high ground level concentrations.

Let P denote the fraction of the plume that penetrates into the elevated stable layer above the mixed layer. This fraction can be calculated by comparing the height of the upper and lower plume edges at final rise, with the height of the mixed layer, h', above the stack:

$$h' = h - h_s \qquad (50)$$

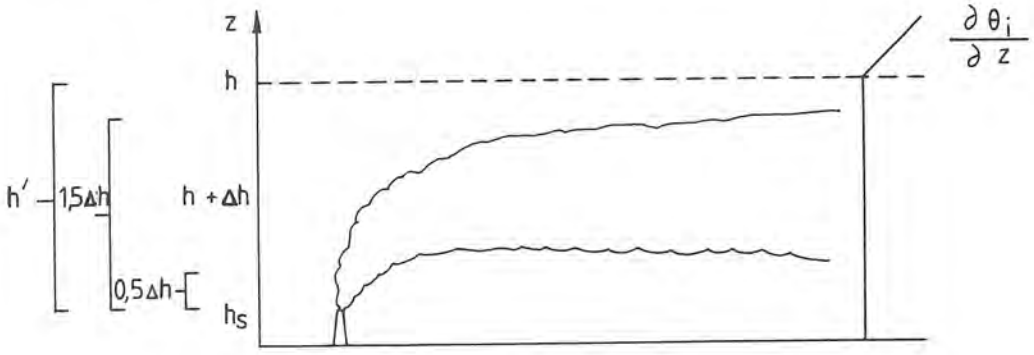

Figure 4 *Length scales used for calculation of plume penetration of an elevated stable layer.*

According to Briggs (1980) the height of the upper and lower plume edges can be approximated by 1.5 Δh and 0.5 Δh respectively. If

$$0.5\,\Delta h \geq h' \qquad (51)$$

the whole plume is above the mixing layer and P = 1. If on the other hand

$$1.5\,\Delta h \leq h' \qquad (52)$$

as in Figure 4, the whole plume is below the mixing layer and P = 0.

Between these cases, when

$$0.5 \leq h'/\Delta h \leq 1.5 \tag{53}$$

the plume partially penetrates the elevated stable layer. The factor P is then given by

$$P = 1.5 - \frac{h'}{\Delta h} \tag{54}$$

The plume fraction remaining within the mixed layer is given by (1-P). Only this part of the plume is here assumed to contribute to ground level concentrations. An effective source strength is introduced by

$$Q'_e = Q(1-P) \tag{55}$$

Following Weil and Brower (1982) the effective source height for the portion of the plume remaining within the mixed layer is

$$h_e = h_s + (0.62 + 0.38P)h' \tag{56}$$

If the final plume rise Δh computed from the 'break up' and 'touch down' models (Eqs (44), (46) and (47)) is larger than $h'/1.5$ the further rise is computed by Briggs' formula for stable stratification (Eq 48) but taking into account that the plume loses a part of its buoyancy when it reaches the height $h'/1.5$. The final plume rise is given by

$$\Delta h = ((2.6)^3 (F/(us_i)) + (h'/1.5)^3)^{1/3} \tag{57}$$

where

$$s_i = \frac{g}{T_a} \frac{\partial \Theta_i}{\partial z} \tag{58}$$

and $\partial\Theta_i/\partial z$ is the potential temperature gradient in the stable layer above the mixing height. Δh in equation (57) is used for calculation of the penetration factor P in (54). For further details see Omstedt (1983).

4. EXPERIMENTS AND RESULTS

Some experiments have been made by using four years of hourly meteorological data and radiosonde data (1978-81) from Bromma airport in Stockholm.

4.1 Stability classification

In Figure 5 a comparison is made between two different stability classification methods. Figure 5(a) shows the frequency distribution of stability class computed by the method used in the present model i.e. the combined method using, w_*/u and the Pasquill-Gifford-Turner (PGT) method. The PGT-method is used during stable conditions, i.e. for hours with negative (downward) sensible heat flux. If the calculated sensible heat flux is negative but the PGT-method gives a neutral or unstable class the PGT-class is changed to neutral. In Figure 5(b) the frequency distribution of stability class using the PGT-method is shown.

An important feature of the stability classification method used in the model is that it gives a greater number of hours with unstable conditions, compared with the PGT-method.

4.2 Dispersion calculations

Ground level concentrations of SO_2 are calculated around a hypothetical 500 MW power plant with emission data given in Table 6. Calculations are made for the four-year time period mentioned above. For each month and in every receptor point 99-percentile ground level concentration values are calculated. These values are of special interest for comparison with the Swedish short-term air quality criterion for SO_2, (see page 1). Examples of results are given in Tables 7 and 8 and corresponding Figures 6 and 7. In Table 7 (Figure 6) the results for the month giving the highest value during the four-year time period show a value of 254 $\mu g/m^3$ at 1750 from the stack. In Table 8 (Figure 7) the results for the month giving the second highest value, give 184 $\mu g/m^3$ at 1250 m from the stack, are shown. Both a tentative comparison of these results with the dispersion model used in Sweden today and a description of it, are given below.

h_s	= 100m	
Q	= 238	g SO_2/s
V_q	= 280	m^3/s
T_q	= 373	^oK

Table 6 Emission data from a hypothetical 500 MW power plant.

h_s is stack height,
Q is emission rate,
V_q is volume flux at stack exit and
T_q is stack exit temperature

4.3 Högström's (1968) model

In Högström's (1968) model statistics of wind direction frequencies and 'dispersion categories' (stability and wind speed) are used as meteorological input data to a Gaussian dispersion model. Dispersion parameters, i.e. σ_y and σ_z, are calculated by formulas derived from an experimental study in Sweden by Högström (1964), mostly under neutral and stable meteorological conditions.

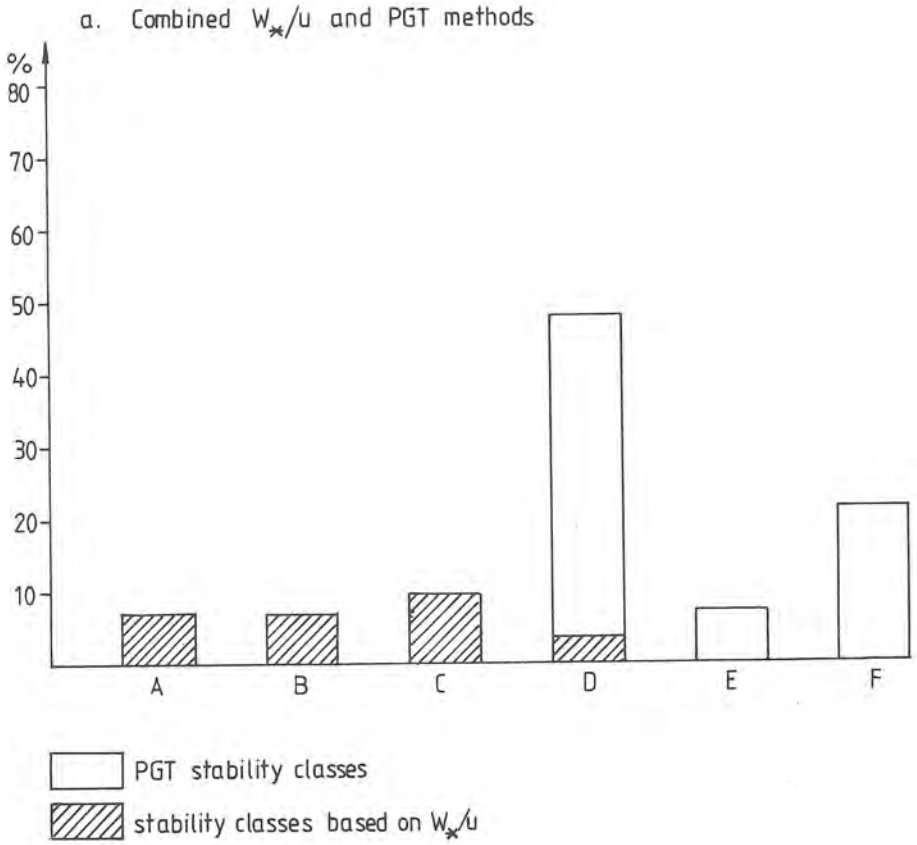

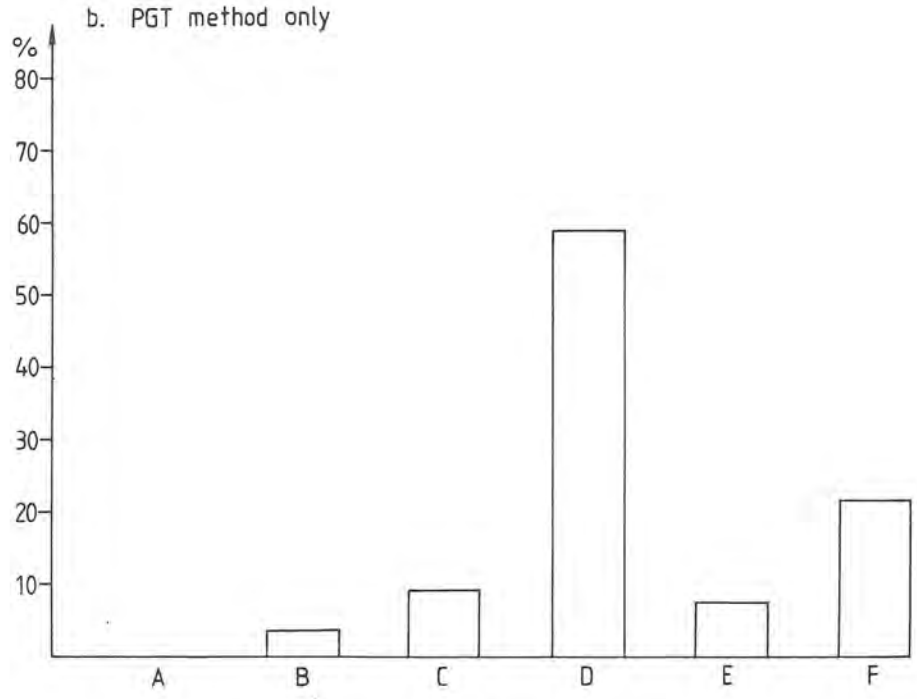

Figure 5 *Frequency distribution of stability class computed by:*

(a) Combined w_*/u and Pasquill-Gifford-Turner (PGT) methods as used in the present model.

(b) PGT-method only.

Four years of hourly meteorological data and radiosonde data from Bromma airport in Stockholm have been used for the computations.

Table 7 *Examples of results from the model using emission data from a hypothetical 500 MW power plant and hourly meteorological data and radiosonde data from Bromma airport in Stockholm. The table shows 99-percentile ground level SO_2-concentration values in $\mu g/m^3$ for the month giving the highest value during a four-year time period (1978-81).*

YEAR:78 MONTH:8
Percentile (%):99
Distance (m)

($\mu g/m^3$)

Wind-direction	500	750	1000	1250	1500	1750	2000	2250	2500	3000	3500	4000	4500	5000	6000
10	9.	35.	58.	72.	78.	75.	72.	69.	67.	64.	58.	50.	43.	37.	28.
20	6.	18.	38.	42.	63.	70.	70.	69.	69.	63.	54.	49.	46.	42.	38.
30	4.	16.	31.	48.	65.	63.	62.	66.	67.	61.	57.	51.	46.	41.	35.
40	2.	9.	22.	33.	39.	43.	41.	41.	40.	37.	34.	31.	27.	24.	19.
50	1.	3.	11.	22.	25.	26.	25.	25.	23.	23.	23.	22.	20.	17.	18.
60	1.	3.	5.	5.	7.	10.	12.	12.	11.	11.	14.	12.	11.	10.	9.
70	1.	3.	3.	4.	4.	4.	4.	4.	3.	4.	4.	5.	5.	5.	5.
80	1.	2.	4.	7.	9.	8.	7.	8.	11.	10.	8.	7.	6.	5.	3.
90	1.	1.	2.	3.	4.	4.	6.	8.	9.	13.	15.	17.	15.	14.	11.
100	1.	1.	3.	5.	6.	5.	5.	6.	8.	12.	17.	18.	17.	16.	16.
110	2.	4.	8.	18.	22.	25.	27.	26.	25.	25.	28.	32.	35.	35.	30.
120	2.	5.	13.	20.	25.	32.	33.	35.	37.	42.	40.	35.	33.	30.	26.
130	4.	12.	23.	30.	36.	44.	51.	55.	57.	52.	49.	48.	45.	40.	36.
140	6.	21.	32.	33.	42.	55.	57.	53.	50.	43.	37.	31.	27.	25.	21.
150	4.	24.	43.	58.	66.	69.	66.	57.	51.	41.	34.	30.	31.	33.	29.
160	5.	17.	31.	42.	48.	49.	50.	49.	48.	47.	43.	39.	35.	31.	26.
170	9.	33.	62.	86.	91.	91.	91.	82.	74.	62.	53.	46.	40.	36.	30.
180	9.	37.	58.	68.	72.	78.	81.	80.	74.	70.	62.	55.	49.	45.	41.
190	13.	36.	64.	66.	70.	73.	70.	63.	59.	47.	42.	40.	38.	36.	30.
200	12.	45.	70.	76.	71.	67.	60.	57.	51.	42.	36.	30.	26.	23.	18.
210	13.	34.	59.	74.	78.	73.	65.	57.	50.	44.	35.	28.	23.	20.	16.
220	11.	37.	50.	60.	62.	61.	57.	52.	49.	41.	35.	30.	25.	22.	18.
230	13.	43.	66.	74.	77.	71.	62.	57.	53.	45.	40.	34.	28.	25.	24.
240	12.	45.	71.	83.	87.	83.	78.	73.	67.	56.	50.	46.	41.	38.	34.
250	10.	37.	69.	76.	72.	68.	68.	68.	67.	61.	54.	48.	43.	39.	33.
260	9.	27.	48.	63.	74.	76.	75.	76.	76.	72.	62.	54.	48.	43.	38.
270	10.	28.	45.	55.	60.	58.	59.	63.	64.	60.	52.	47.	43.	40.	34.
280	11.	34.	67.	92.	98.	91.	83.	82.	80.	74.	70.	66.	57.	53.	45.
290	24.	68.	95.	115.	149.	174.	188.	192.	176.	158.	144.	128.	115.	105.	89.
300	27.	105.	193.	223.	245.	254.	252.	251.	229.	194.	169.	153.	144.	132.	113.
310	42.	130.	181.	196.	201.	191.	169.	156.	143.	120.	103.	91.	82.	73.	61.
320	29.	76.	116.	145.	169.	158.	141.	128.	126.	117.	102.	90.	82.	74.	64.
330	11.	37.	68.	92.	93.	96.	90.	85.	82.	71.	61.	53.	46.	41.	34.
340	13.	33.	59.	76.	76.	74.	73.	66.	59.	48.	39.	34.	36.	34.	28.
350	8.	30.	59.	73.	78.	76.	74.	70.	71.	61.	52.	47.	41.	39.	38.
360	11.	39.	67.	76.	75.	72.	73.	73.	66.	58.	54.	49.	45.	41.	34.

Max conc: 254 $\mu g/m^3$
Distance: 1750 m
Wind direction: 300°

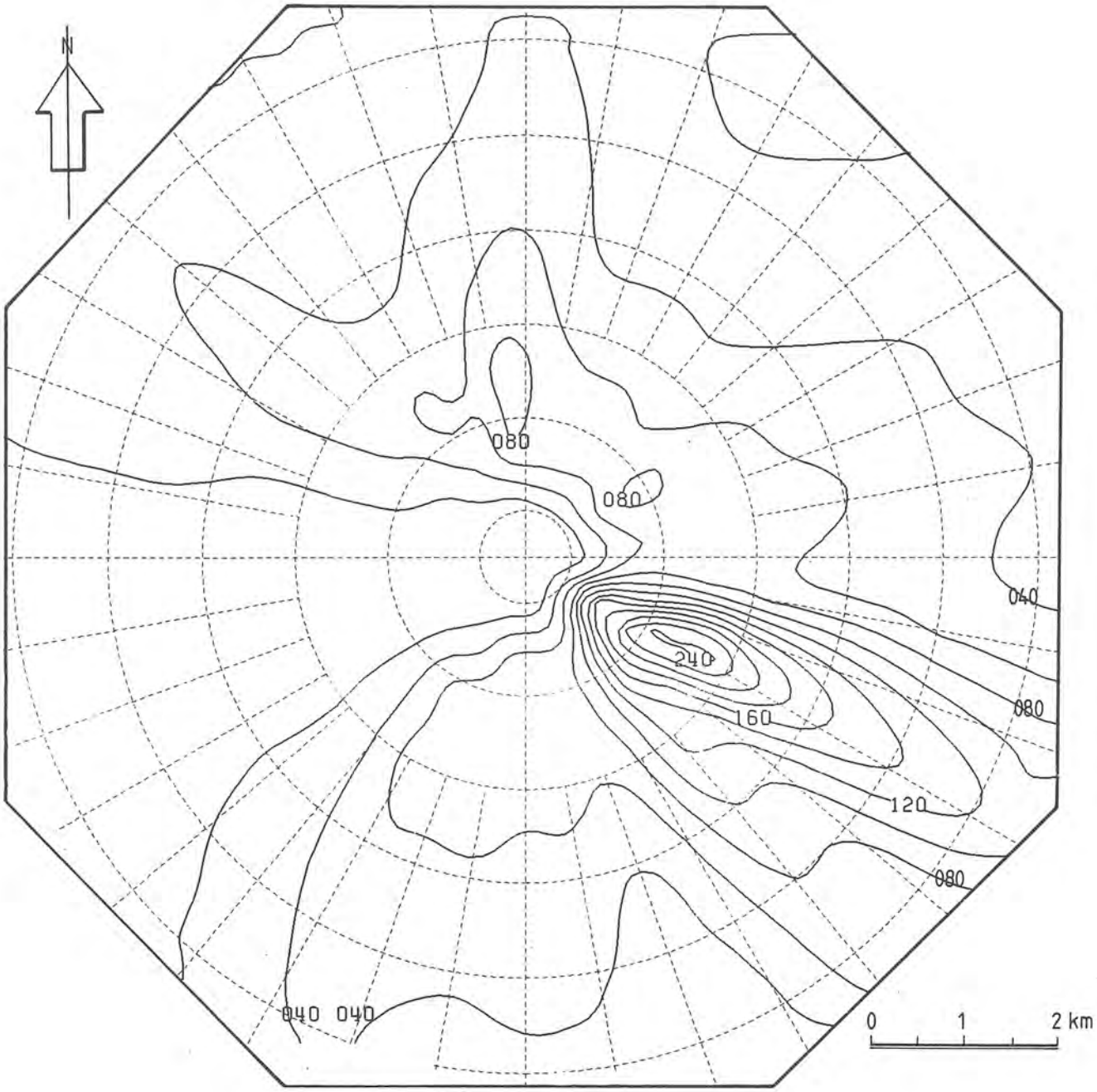

Figure 6 *The geographical distribution of 99-percentile ground level SO_2-concentration values in $\mu g/m^3$ as obtained in Table 7.*

Table 8 As Table 7 but for the month giving the second highest value during a four-year time period (1978-81).

YEAR:79 MONTH:6
Percentile (%):99
Distance (m)

($\mu g/m^3$)

Wind-direction	500	750	1000	1250	1500	1750	2000	2250	2500	3000	3500	4000	4500	5000	6000
10	14.	44.	55.	60.	61.	59.	57.	54.	50.	42.	34.	29.	25.	22.	17.
20	11.	34.	44.	41.	44.	46.	46.	48.	49.	38.	30.	24.	20.	17.	13.
30	6.	25.	40.	45.	44.	43.	37.	34.	30.	25.	22.	19.	17.	15.	12.
40	3.	14.	17.	28.	36.	40.	40.	35.	32.	27.	24.	23.	19.	16.	13.
50	2.	6.	12.	24.	23.	22.	18.	16.	14.	12.	12.	11.	9.	8.	6.
60	1.	3.	9.	10.	10.	9.	8.	7.	6.	4.	3.	2.	2.	2.	1.
70	1.	3.	7.	8.	7.	6.	5.	5.	4.	3.	2.	2.	2.	1.	1.
80	2.	7.	20.	33.	32.	31.	29.	27.	24.	19.	15.	13.	11.	9.	7.
90	2.	9.	20.	35.	47.	54.	50.	45.	41.	34.	29.	26.	23.	21.	16.
100	8.	14.	21.	26.	31.	32.	28.	29.	28.	23.	18.	15.	12.	11.	8.
110	7.	22.	33.	35.	33.	28.	24.	21.	20.	17.	16.	14.	12.	10.	10.
120	5.	27.	38.	35.	35.	44.	49.	48.	41.	34.	26.	22.	23.	20.	20.
130	11.	36.	47.	54.	64.	65.	60.	58.	51.	50.	42.	36.	31.	27.	21.
140	21.	52.	57.	57.	57.	60.	54.	48.	46.	45.	43.	41.	39.	36.	30.
150	15.	45.	68.	62.	66.	70.	72.	72.	65.	56.	48.	42.	38.	34.	27.
160	16.	49.	69.	76.	74.	71.	64.	60.	56.	53.	41.	36.	35.	34.	29.
170	24.	68.	66.	72.	59.	62.	59.	60.	58.	49.	41.	35.	31.	29.	24.
180	30.	63.	100.	107.	103.	90.	80.	73.	66.	62.	56.	49.	43.	39.	33.
190	41.	81.	104.	110.	104.	103.	100.	91.	83.	69.	60.	54.	48.	44.	43.
200	49.	115.	118.	108.	117.	117.	122.	118.	113.	101.	88.	78.	70.	64.	55.
210	52.	127.	181.	182.	158.	157.	155.	144.	133.	119.	104.	92.	83.	76.	64.
220	38.	86.	109.	130.	134.	131.	124.	114.	103.	87.	76.	67.	60.	53.	42.
230	25.	74.	104.	128.	122.	107.	94.	101.	107.	87.	71.	58.	52.	47.	41.
240	19.	60.	86.	87.	86.	85.	81.	75.	70.	61.	55.	51.	45.	40.	34.
250	14.	42.	70.	76.	73.	67.	62.	63.	64.	56.	52.	46.	42.	38.	32.
260	13.	49.	78.	85.	85.	77.	70.	63.	57.	46.	45.	43.	39.	37.	31.
270	11.	39.	64.	74.	75.	72.	66.	59.	52.	48.	44.	40.	36.	32.	26.
280	17.	49.	72.	73.	73.	74.	68.	61.	55.	45.	38.	33.	31.	29.	24.
290	13.	41.	67.	73.	72.	72.	70.	64.	59.	49.	42.	36.	33.	30.	26.
300	9.	23.	43.	71.	88.	80.	73.	72.	71.	60.	50.	43.	37.	33.	27.
310	9.	30.	43.	65.	75.	74.	77.	73.	70.	64.	54.	47.	41.	37.	31.
320	12.	34.	55.	55.	60.	62.	54.	52.	48.	50.	51.	46.	41.	38.	34.
330	13.	40.	51.	60.	58.	61.	57.	52.	44.	35.	28.	23.	22.	22.	20.
340	26.	62.	69.	73.	72.	61.	53.	48.	43.	32.	26.	23.	20.	18.	14.
350	22.	56.	73.	67.	64.	61.	55.	48.	42.	32.	27.	22.	18.	16.	12.
360	16.	53.	75.	78.	75.	68.	60.	56.	54.	48.	44.	39.	34.	31.	26.

Max conc: 182 $\mu g/m^3$
Distance: 1250 m
Wind direction: 210°

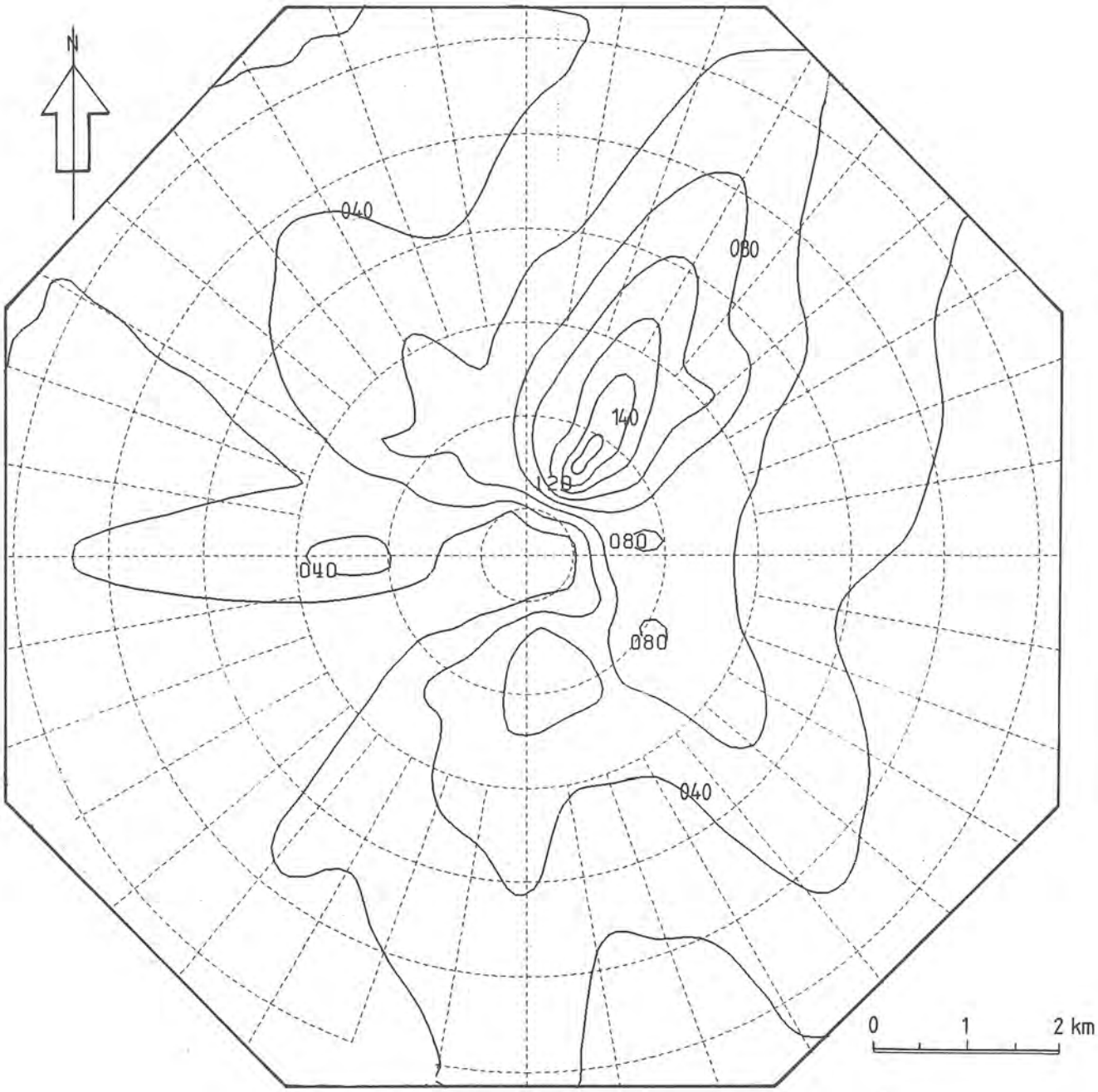

Figure 7 The geographical distribution of 99-percentile ground level SO_2-concentration values in $\mu g/m^3$ as obtained in Table 8.

Plume rise is calculated by empirical formulae developed by Bringfelt (1968, 1969). The plume rise data i.e.photographs of smoke from Swedish industrial smoke stacks, were also taken mostly under neutral and stable meteorological conditions.

The model was tested against a continuous record of ground level concentration values obtained at one point 750 m from a sulphuric acid plant in southern Sweden. The heat flux of the stack gases from the dominating plant was of about 1 MW.

Högström's (1968) model has been used in Sweden since the 1960's in different regulatory applications. In almost all applications statistics of 'dispersion categories' (stability and wind speed) are obtained from 30 months of data from Ågesta (mast data) or 47 months of data from Torslanda (radiosonde data).

The model has recently been tested against measured ground level SO_2 concentrations, from tall stacks in the USA. This shows that the ground level concentrations during convective meteorological conditions predicted by this model are too high (Omstedt, 1982).

In this report a tentative comparison between Högtröm's model and the present model is made for predicted 99-percentile ground level SO_2-concentration values. The same emission data are used (Table 6), which implies a heat content of the stack gases of about 24 MW, but using different meteorological data. In Högtröm's model statistics of 'dispersion categories' from Ågesta (mast data) during 1960-03--1962-08 and statistics of wind direction frequencies from Bromma airport (near Ågesta) during the same time period are used. The results are given in Table 9 for the month giving the highest 99-percentile ground level SO_2-concentration value, i.e. 462 $\mu g/m^3$ at 750 m, during the 30 month time period mentioned above. This table can be compared with corresponding results obtained from the present model (Table 7) showing that Högström's model predicts a factor 1.8 higher maximum 99-percentile ground level concentration value and that this value is obtained at a closer distance from the stack, compared with results from the present model. This conclusion is of course only valid for this special case and under the assumptions given above. These results are, however, consistent with results given by Omstedt (1982), indicating that Högström's model overestimates the highest 99-percentile ground level concentration values and that they are obtained at distances too close to tall industrial stacks.

4.4 Future improvements of the model

Future work will be directed towards the following improvements.

1. Incorporation of w_*/u_* directly into the expression for σ_y and σ_z. The advantage of this approach is to give the variables a continuous variation of stability, as actually occurs in the atmosphere, rather than lumping them together in discrete classes.

2. Incorporation of dispersion parameters for low sources, i.e. sources with effective stack heights less than 0.1 h.

3. Improvements of the parameterization of the stable boundary layer to replace the PGT-method used in the model.

Percentile (%): 99 ($\mu g/m^3$)

Wind-direction \ Distance (m)	500	750	1000	1250	1500	1750	2000	2250	2500	3000	3500	4000	4500	5000	6000
N	269	308	228	200	166	137	121	109	95	82	69	57	53	43	35
NE	52	62	52	48	50	41	39	37	33	27	25	21	16	14	11
E	269	308	228	200	166	137	121	109	94	82	69	57	53	43	35
SE	200	216	168	144	123	111	99	90	82	67	57	50	44	36	28
S	346	433	320	291	228	190	160	143	125	110	87	76	65	67	62
SW	356	450	331	304	236	202	165	150	135	114	90	81	71	73	69
W	363	462	339	314	242	210	169	155	142	117	91	85	76	78	73
NW	299	355	268	233	191	157	134	120	105	90	76	62	57	49	41

Max conc: 462 $\mu g/m^3$
Distance: 750 m
Wind direction: W

Table 9 *By Högström's model (1968) calculated 99-percentile ground level SO_2-concentration values in $\mu g/m^3$ using emission data from a hypothetical 500 MW power plant. The table shows the values for the month giving the highest value during a 30 month time period.*

5. SUMMARY AND CONCLUSIONS

An operational air pollution model using routine meteorological data is described. An hourly time series of pollutant concentrations is calculated for emissions from one or several tall industrial stacks. New methods developed by Nielsen et al. (1981), Berkowicz and Prahm (1982 a, b), Olesen et al. (1983) are used for determining boundary layer parameters i.e. surface sensible heat flux, friction velocity, mean wind speed and mixing height. These parameter values are used as input data to the dispersion part of the model. An updated Gaussian dispersion model, strongly supported by experimental data and similar to that developed by Weil and Bower (1982) is used. Briggs' dispersion parameters are used with the stability classification scheme based on the values of w_*/u during daytime and Pasquill-Gifford-Turner classes during nighttime for selection of stability classes. Plume rise and plume penetration of elevated stable layers are calculated by formulae from Briggs (1975). A similar model will also be used in Denmark (Berkowicz et al., 1983). Examples of results are given, based on four years of hourly meteorological data and radiosonde data from Bromma airport in Stockholm. A tentative comparison between the present model and Högström's (1968) model is made for emission from a 500 MW power plant. This comparison indicates that Högström's model predicts ground level concentrations that are too high occurring too close to tall industrial stacks.

6. ACKNOWLEDGEMENT

This work has been sponsored by AB Svarthålsforsen, Statens Vattenfall, Sydkraft and SMHI.

I wish to thank Björn Bringfelt, Sture Ring and Christer Persson for their interest and support of this work. Special thanks are due to the staff of the Danish Air Pollution Laboratory for useful discussions and helpfulness during my visit there. I also wish to thank Christina Lindgren for writing several of the computer programs, Svante Bodin for the review of this report and Kerstin Fabiansen for typing the manuscript.

7. REFERENCES

Berkowicz, R. and Prahm, L.P., 1982a: Sensible heat flux estimated from routine meteorological data by the resistance method. J. Appl. Met. 21, 1845-1864.

Berkowicz, R. and Prahm, L.P., 1982b: Evaluation of the profile method for estimation of surface fluxes of momentum and heat. Atm. Env. 16, 2809-2819.

Berkowicz, R., Baerentsen, J.H., Jensen, A.B., Markvorsen, J.S., Nielsen, L.B., Olesen, H.R., Prahm, L.P., 1983: An operational air pollution model. 14th International Technical Meeting on Air Pollution Modeling and Its Application. NATO/CCMS, Copenhagen.

Briggs, G.A., 1975: Plume rise predictions.In Lectures on Air Pollution and Environmental Impact Analyses. American Meteorological Society, Boston, Ma.

Briggs, G.A., 1980: Plume rise and buoyancy effects. In Atmospheric Science and Power Production, Atmospheric Turbulence and Diffusion Laboratory, NOAA, Oak Ridge, Tn.

Bringfelt, B., 1968: Plume rise measurements at industrial chimneys. Atm. Env, 2, 575-598.

Bringfelt, B.,1969: A study of buoyant chimney plumes in neutral and stable atmospheres. Atm. Env, 3, 609-623.

Brutsaert, W., 1975: Comments on surface roughness parameters and the height of dense vegetation. J. Meteor. Soc., Japan, 53, 96-97.

Businger, J.A., Wyngaard, J.C., Izumi,Y., Bradley, E.F., 1971: Flux profile relationships in the atmospheric surface layer. J. Atm. Sci. 28, 181-189.

Carpenter, S.B., Leavitt, J.M., Colbaugh, W.C., Thomas, F.W., 1970: Principal plume dispersion models at TVA power plants. Paper presented at 63rd Annual Meeting of the Air Pollution Association, St Louis, Mo, Paper No 70-149.

Carson, D.J., 1973: The development of a dry inversion-capped convectively unstable boundary layer. Quart. J. R. Met. Soc. 99, 450-467.

Driedonks, A.G.M., 1982: Models and observations of the growth of the atmospheric boundary layer. Bound.-layer Meteor., 23, 283-306.

Deardorff, J.W., 1972: Numerical investigation of neutral and unstable planetary boundary layers. J. Atmos. Sci., 29, 91-115.

Gifford, F.A., 1961: Uses of routine meteorological observations for estimating atmospheric dispersion. Nuclear Safety 2, 47-51.

Gifford, F.A., 1975: Atmospheric dispersion models for environmental pollution applications. In Lectures on Air Pollution and Environmental Impact Analyses. American Meteorological Society, Boston, Ma.

Haugen, D.A., 1959: Project Prairie Grass, a field programme in diffusion. Geophysical Research Paper, 59, Vol. III.

Högström, U., 1964: An experimental study on atmospheric diffusion. Tellus 16 (2), 205.

Högström, U., 1968: A statistical approach to the air pollution problem of chimney emission. Atm. Env. 2, 251-271.

Kaimal, J.C., Wyngaard, J.C., Haugen, D.A., Coté, O.R., Izumi, Y., Caughey, S.J. and Readings, C.J., 1976: Turbulence structure in the convective boundary layer. J. Atmos. Sci. 33, 2152-2169.

Misra, P.K., 1982: Dispersion of non-buoyant particles inside a convective boundary layer. Atmos. Environ. 16: 239-243.

Monin, A.S. and Obukhov, A.M., 1954: Dimensionless characteristics of turbulence in the atmospheric surface layer. Dokl. Akad. Nauk. SSSR 93, 223-226.

Monteith, J.L., 1965: Evaporation and environment. In The State and Movement of Water in Living Organisms, 19th Symposium, Soc. Exp. Biol., 205-235.

Monteith, J.L. and Szeicz, G., 1961: The radiation balance of bare soil and vegetation. Quart. J.R. Met. Soc. 87, 159.

Nielsen, L.B., Prahm, L.P., Berkowicz, R. and Conradsen, K., 1981: Net incoming radiation estimated from hourly global radiation and/or cloud observations. J. Climat. 1, 255-272.

Olesen, H.R., Jensen, A.B. and Brown, N., 1983: Operational procedure for estimation of mixing height for air pollution models (in preparation).

Omstedt, G., 1982: Spridning av luftföroreningar från skorstenar i konvektiva gränsskikt. Swedish Meteorological and Hydrological Institute, RMK 37.

Omstedt, G., 1983: En undersökning av "The Maryland PPSP dispersion model for tall stacks". Swedish Meteorological and Hydrological Institute. FoU-Notis Nr 23.

Pasquill, F., 1961: The estimation of the dispersion of windborne material. Meteorol. Mag. 90, 33-49.

Pasquill, F., 1976: Atmospheric parameters in Gaussian plume modeling. Part II: Possible requirements for change in the Turner workbook values. U.S. Environmental Protection Agency. Ref. No. EPA-600/4-76-0306.

Robertson, G.W. and Russel, D.A., 1968: Astrometeorological Estimator. Ag. Met. Tech. Bull. No. 14, Agromet Section, Plant Research Institute, C.E.F. Ottawa 3, Ontario, Canada, 22 pp.

Singer, I.A. and Smith, M.E., 1966: Atmospheric diffusion at Brookhaven National Laboratory. Int. J. Air Water Pollut. 10,125-135.

Taylor, G.I., 1921: Diffusion by continuous movements. Proc. London Math. Soc., Ser. 2, 20, 196-202.

Tennekes, H., 1973: A model for the dynamics of the inversion above a convective boundary layer. J. Atm. Sci. 30, 558-567.

Tennekes, H. and Driedonks, A.G.M., 1981: Basic entrainment equations for the atmospheric boundary layer. Bound.-Layer Meteor., 20., 515-531.

Turner, B., 1964: A diffusion model for an urban area. J. Appl. Met. 3, 83-91.

Turner, B., 1980: Problems connected with the evaluation of dispersion of air pollutants from major sources. Lectures hold at Korpilampi, Finland.

Venkatram, A., 1980: Estimating the Monin-Obukhov length in the stable boundary layer for dispersion calculations. Bound.-Layer Meteor., 19., 481-485.

Venkatram, A., 1983: On dispersion in the convective boundary layer. Atm. Env. 17, 529-533.

Weil, J.C. and Furth, W.F., 1981: A simplified numerical model of dispersion from elevated sources in the convective boundary layer, pp 76-77 in Proceedings Fifth Symposium on Turbulence, Diffusion and Air Pollution. Atlanta, GA. American Meteorological Society, Boston, MA.

Weil, J.C. and Brower, R.P., 1982: The Maryland PPSP dispersion model for tall stacks. PPSP-MP-36, Martin Marietta Corp., Environmental Center, Balmore, Md 21227.

Weil, J.C. and Brower, R.P., 1983: Estimating convective boundary layer parameters for diffusion applications. PPSP-MP-48, Martin Marietta Corp., Environmental Center, Baltimore, Md 21227.

Willis, G.E. and Deardorff, J.W., 1974: A laboratory model of the unstable planetary boundary layer. J. Atmos. Sci., 31, 1297-1307.

APPENDIX A

The Gaussian equation and grid systems used.

Two different grid systems are used. For single source calculations a polar coordinate system is used. The down wind distance, x, and the crosswind distance, y, from the point source to a receptor are given by

$$x = x$$
$$y = \frac{\Delta\Theta}{180}\,\Pi \cdot x \qquad \text{(A1)}$$

where $\Delta\Theta$ is the angle between the wind direction and the receptor point. Examples of results using this grid system are shown in Table 7 and Figure 6.

For multiple source calculations a cartesian coordinate system is used. Let x and y denote the downwind distance and the crosswind distance respectively from a point source to a receptor. The grid transformation is then given by:

$$x = (x_r - x_s)\cos\Theta + (y_r - y_s)\sin\Theta$$
$$y = -(x_r - x_s)\sin\Theta + (y_r - y_s)\cos\Theta \qquad \text{(A2)}$$

where (x_s, y_s) are the coordinates of a point source
(x_r, y_r) are the coordinates of a receptor and
Θ is the mathematical wind direction, (i e anti-clockwise with wind blowing from west as zero).

The contribution to the concentration c(x,y,z) from a single point source to a receptor is given by one of the two following equations:

$$c(x,y,z) = \frac{Q}{u}\,\frac{g_1}{\sqrt{2\Pi}\sigma_y} \cdot \frac{g_2}{\sqrt{2\Pi}\sigma_z} \qquad \text{(A3)}$$

$$c(x,y,z) = \frac{Q}{u}\,\frac{g_1}{\sqrt{2\Pi}\sigma_y} \cdot \frac{1}{h} \qquad \text{(A4)}$$

where Q is emission rate,
u is wind speed,
σ_y is standard deviations of plume concentration horizontal distribution,
σ_z is standard deviation of plume concentration vertical distribution and
h is the mixing height

The expressions g_1 and g_2 are given by:

$$g_1 = \exp\ (-0.5\ y^2/\sigma_y^2) \qquad \text{(A5)}$$

$$g_2 = \sum_{N=-\infty}^{\infty} \{\exp(-0.5(z-H+2Nh)^2/\sigma_z^2) + \exp(-0.5(z+H+2Nh)^2/\sigma_z^2)\} \qquad \text{(A6)}$$

where H is the effective source height and
z is the receptor height above ground.

If the vertical concentration distribution is uniform within the mixing layer, equation (A4) is used. Sensitivity tests of equation (A3) have shown that for all values of H and z between the ground and mixing height, the vertical concentration distribution is uniform when σ_z has increased to 1.6 h. For ground level receptors equation (A4) may give appropriate concentrations for σ_z = 0.8 h (Turner, 1980).

Figure A1 shows results using the quadratic grid system (eq A2). This figure can be compared with corresponding results using the polar coordinate system (eq A1) in Figure 6. Two different computer programs for plotting concentration lines have been used.

YEAR:78 MONTH:8
Percentile (%):99

A:3

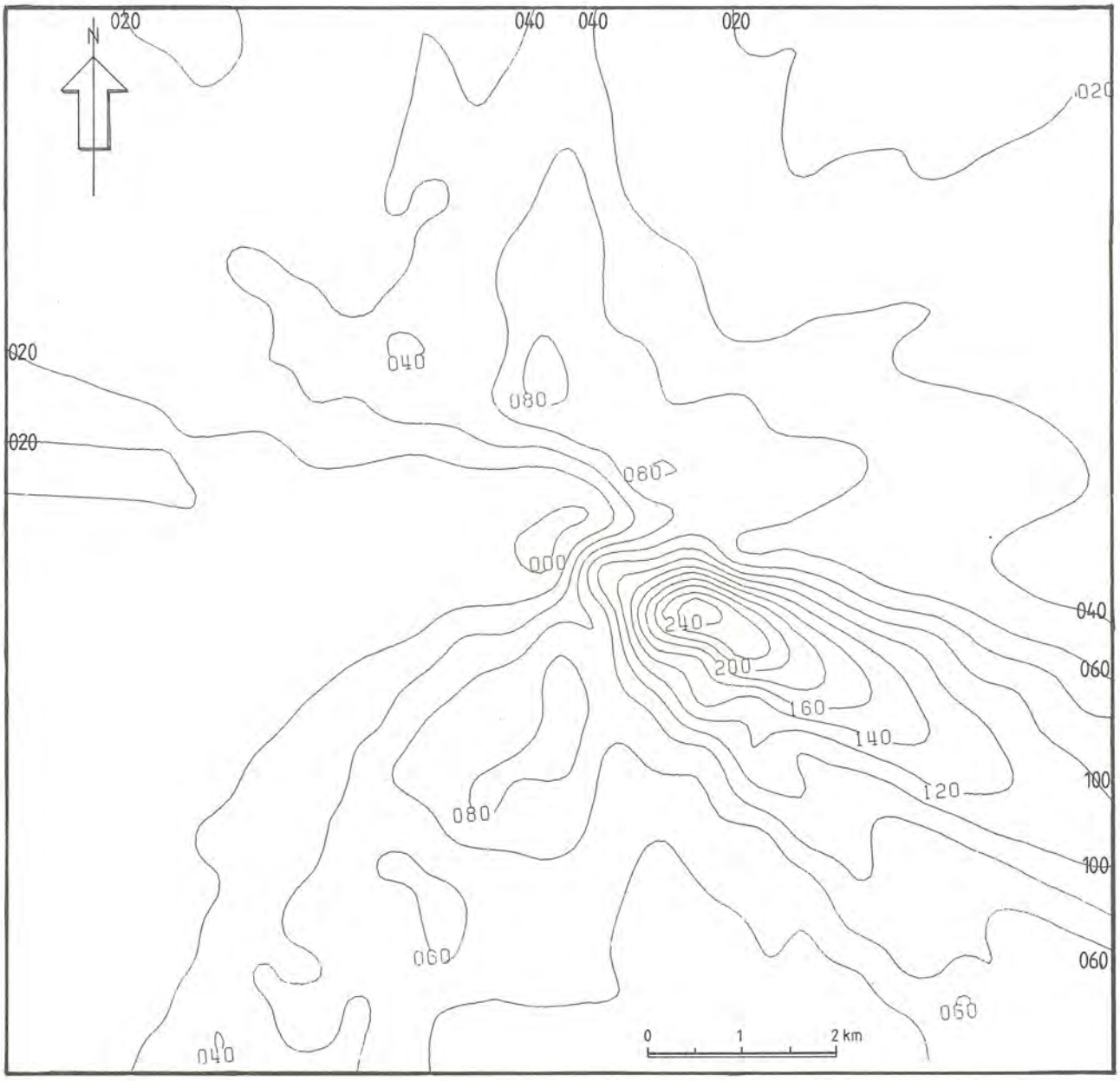

Figure A1 *Examples of results from the model using the cartesian grid system (Eq. A2) with emission data from a hypothetical 500 MW power plant (Table 6) and hourly meteorological data and radiosonde data from Bromma airport in Stockholm. The figure shows 99-percentile ground level SO_2-concentration values in $\mu g/m^3$ for the month giving the heighest value during a four-year time period (1978-81).*

SMHI Rapporter, METEOROLOGI OCH KLIMATOLOGI (RMK)

Nr 1 Thompson, T, Udin, I and Omstedt, A
Sea surface temperatures in waters surrounding Sweden. (1974)

Nr 2 Bodin, S
Development on an unsteady atmospheric boundary layer model. (1974)

Nr 3 Moen, L
A multi-level quasi-geostrophic model for short range weather predictions. (1975)

Nr 4 Holmström, I
Optimization of atmospheric models. (1976)

Nr 5 Collins, W G,
A parameterization model for calculation of vertical fluxes of momentum due to terrain induced gravity waves. (1976)

Nr 6 Nyberg, A
On transport of sulphur over the North Atlantic. (1976)

Nr 7 Lundqvist, J-E and Udin, I
Ice accretion on ships with special emphasis on Baltic conditions. (1977)

Nr 8 Eriksson, B
Den dagliga och årliga variationen av temperatur, fuktighet och vindhastighet vid några orter i Sverige. (1977)

Nr 9 Holmström, I and Stokes, J
Statistical forecasting of sea level changes in the Baltic. (1978)

Nr 10 Omstedt, A and Sahlberg, J
Some results from a joint Swedish-Finnish Sea Ice Experiment, March, 1977. (1978)

Nr 11 Haag, T
Byggnadsindustrins väderberoende, seminarieuppsats i företagsekonomi, B-nivå. (1978)

Nr 12 Eriksson, B
Vegetationsperioden i Sverige beräknad från temperaturobservationer. (1978)

Nr 13 Bodin, S
En numerisk prognosmodell för det atmosfäriska gränsskiktet grundad på den turbulenta energiekvationen.

Nr 14 Eriksson, B
Temperaturfluktuationer under senaste 100 åren. (1979)

Nr 15 Udin, I och Mattisson, I
Havsis- och snöinformation ur datorbearbetade satellitdata - en modellstudie. (1979)

Nr 16 Eriksson, B
Statistisk analys av nederbördsdata. Del I.
Arealnederbörd(1979)

Nr 17 Eriksson, B
Statistisk analys av nederbördsdata. Del II.
Frekvensanalys av månadsnederbörd. (1980)

Nr 18 Eriksson, B
Årsmedelvärden (1931-60) av nederbörd, avdunstning och avrinning. (1980)

Nr 19 Omstedt, A
A sensitivity analysis of steady, free floating ice.
(1980)

Nr 20 Persson, C och Omstedt, G
En modell för beräkning av luftföroreningars spridning och deposition på mesoskala (1980)

Nr 21 Jansson, D
Studier av temperaturinversioner och vertikal vindskjuvning vid Sundsvall-Härnösands flygplats (1980)

Nr 22 Sahlberg, J and Törnevik, H
A study of large scale cooling in the Bay of Bothnia
(1980)

Nr 23 Ericson, K and Hårsmar, P-O
Boundary layer measurements at Klockrike. Oct 1977 (1980)

Nr 24 Bringfelt, B
A comparison of forest evapotranspiration determined by some independent methods (1980)

Nr 25 Bodin, S and Fredriksson, U
Uncertainty in wind forecasting for wind power networks
(1980)

Nr 26 Eriksson, B
Graddagsstatistik för Sverige (1980)

Nr 27 Eriksson, B
Statistisk analys av nederbördsdata. Del III 200-åriga nederbördsserier. (1981)

Nr 28 Eriksson, B
Den "potentiella" evapotranspirationen i Sverige (1981)

Nr 29 Pershagen, H
Maximisnödjup i Sverige (perioden 1905-70) (1981)

Nr 30 Lönnqvist, O
Nederbördsstatistik med praktiska tillämpningar (Precipitation statistics with practical applications) (1981)

Nr 31 Melgarejo, JW
Similarity theory and resistance laws for the atmospheric boundary layer (1981)

Nr 32 Liljas, E
Analys av moln och nederbörd genom automatisk klassning av AVHRR data (1981)

Nr 33 Ericson, K
Atmospheric Boundary Layer Field Experiment in Sweden 1980, GOTEX II, part I (1982)

Nr 34 Schoeffler, P
Dissipation, dispersion and stability of numerical schemes for advection and diffusion (1982)

Nr 35 Undén, P
The Swedish Limited Area Model (LAM). Part A. Formulation (1982)

Nr 36 Bringfelt, B
A forest evapotranspiration model using synoptic data (1982)

Nr 37 Omstedt, G
Spridning av luftföroreningar från skorstenar i konvektiva gränsskikt (1982)

Nr 38 Törnevik, H
An aerological model for operational forecast of pollen concentration in the air (1982)

Nr 39 Omstedt, G
An operational air pollution model using routine meteorological data

SMHI

SWEDISH METEOROLOGICAL AND HYDROLOGICAL INSTITUTE
Box 923, S-601 19 Norrköping, Sweden. Phone +46 11 10 80 00. Telex 644 00 smhi s